


Dirac Surface States in Magnonic Analogs of Topological Crystalline Insulators

Hiroki Kondo^{✉*} and Yutaka Akagi[✉]

Department of Physics, Graduate School of Science, The University of Tokyo, 7-3-1 Hongo, Tokyo 113-0033, Japan

 (Received 7 December 2020; revised 6 September 2021; accepted 21 September 2021; published 20 October 2021)

We propose magnonic analogs of topological crystalline insulators which possess Dirac surface states protected by the combined symmetry of time reversal and half translation. Constructing models of the topological magnon systems, we demonstrate that an energy current flows through the systems in response to an electric field, owing to the Dirac surface states with the spin-momentum locking. We also propose a realization of the magnonic analogs of topological crystalline insulators in the magnetic compound CrI_3 with a monoclinic structure.

DOI: [10.1103/PhysRevLett.127.177201](https://doi.org/10.1103/PhysRevLett.127.177201)

Introduction.—There has been an explosion of interest in the topological properties of condensed matter systems [1–8], especially since the proposal of topological insulators (TIs) [9–11] robust against perturbations such as disorder [12–29]. One of their hallmarks is the appearance of the Dirac surface states protected by time-reversal symmetry. During the last decade, it has been recognized that crystalline symmetries lead to a more refined classification of phases, so-called topological crystalline insulators (TCIs) [30–33]. Among them, of particular interest are antiferromagnetic topological insulators [34], known as one of the earliest proposals of TCIs. They can be roughly regarded as a stack of quantum Hall insulators with alternating Chern numbers. They have Dirac surface states topologically protected by the combined symmetry of time reversal and translation of half a unit cell in the stacking direction.

Topological phases and phenomena have also been explored intensively in bosonic systems such as systems of magnons [35–52], photons [53–59], phonons [60–71], triplons [72–76,125], and Bose-Einstein condensates [78–86]. The topological classification is more complicated than that in fermionic systems because bosonic Bogoliubov–de Gennes (BdG) systems possess non-Hermiticity due to Bose statistics [87–89]. Meanwhile, topological bosonic systems can exhibit fascinating transport phenomena which are qualitatively different from those in fermionic systems. For example, in the magnonic Weyl semimetals [90–94], magnons having no electric charge can be driven by an electric field due to the chiral anomaly. As examples of symmetry-protected topological phases for bosons, magnonic analogs of quantum spin Hall insulators [95–97]

and three-dimensional TIs [98] were proposed recently. However, the latter system possessing a single surface Dirac state is quite artificial; i.e., the system is a kind of a “bilayer” diamond lattice which is constructed so that they have pseudo-time-reversal symmetry [99]. Hence, its realization in real materials seems to be difficult.

In this Letter, we construct a model of a three-dimensional magnet which has single magnon Dirac surface states protected by the symmetry of the combined operation of time reversal (Θ) and half translation ($T_{1/2}$). We represent the combined operator as $S = \Theta T_{1/2}$ and refer to the symmetry as S symmetry. The model describes a magnonic analog of antiferromagnetic topological insulators (MAFTIs) [34] or TCIs. Since magnons are bosons, the time-reversal operator squares to the identity, which does not ensure the existence of Kramers pairs. On the other hand, S symmetry leads to Kramers degeneracy at certain wave vectors, at which topologically protected surface Dirac states can exist.

In addition, we show that a homogeneous electric field induces the imbalance of the position of the surface Dirac cones between opposite surfaces in MAFTIs, which gives rise to an energy current. Owing to the Aharonov-Casher (AC) effect [100] and the spin-momentum locking [101–103] in the magnon surface states, the system exhibits such an intrinsic electric-field response whose counterpart is absent in electronic systems. We evaluate the energy current driven by an electric field by using linear response theory. As an advantage of the concept for MAFTIs, we also propose that the magnetic compound CrI_3 [104–112] with a monoclinic structure is a candidate material for MAFTIs.

Models.—As a model for MAFTIs, we consider a stack of honeycomb lattice magnets with intralayer ferromagnetic and interlayer antiferromagnetic interactions, where the spins on the same layer (odd and even layers) are aligned in the same direction (opposite directions) [see Fig. 1]. The Hamiltonian is given as follows:

Published by the American Physical Society under the terms of the Creative Commons Attribution 4.0 International license. Further distribution of this work must maintain attribution to the author(s) and the published article's title, journal citation, and DOI.

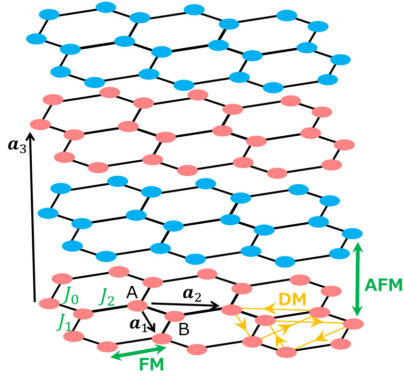


FIG. 1. Stacked honeycomb lattice magnet. Red and blue circles represent spins pointing in the $+z$ and $-z$ directions, respectively. The two sublattices of each layer are indicated by A and B. The three bond-dependent couplings are represented by J_n ($n = 0, 1, 2$). The orange arrows indicate the sign convention $\xi_{ij} = +1 (= -\xi_{ji})$ for $i \rightarrow j$. The vectors \mathbf{a}_1 , \mathbf{a}_2 , and \mathbf{a}_3 are the lattice primitive vectors of the lattice.

$$\mathcal{H} = -\sum_{\langle ij \rangle, l} \mathbf{S}_{i,l} J_{ij} \mathbf{S}_{j,l} + D \sum_{\langle\langle ij \rangle\rangle, l} \xi_{ij} (\mathbf{S}_{i,l} \times \mathbf{S}_{j,l})_z + J' \sum_{i, (l, l')} \mathbf{S}_{i,l} \cdot \mathbf{S}_{i, l'} \quad (1)$$

Here, $\mathbf{S}_{j,l}$ is given by $\mathbf{S}_{j,l} := (S_{j,l}^x, S_{j,l}^y, S_{j,l}^z)$, where $S_{j,l}^\gamma$ is the γ component ($\gamma = x, y, z$) of the spin operator. The subscripts i, j and l, l' are the labels for the sites in honeycomb lattices and for the layers, respectively. Here, the first term is the nearest-neighbor ferromagnetic Heisenberg interaction with bond dependence and XYZ anisotropy. The bond-dependent matrix J_{ij} is a 3 by 3 diagonal matrix $J_{ij} := J_n = \text{diag}(J_n^x, J_n^y, J_n^z)$ ($n = 0, 1, 2$) for the three different bonds $\langle ij \rangle$ in the honeycomb lattice shown in Fig. 1. The second term represents the Dzyaloshinskii-Moriya (DM) interaction between next-nearest neighbor sites, where ξ_{ij} is a sign convention described by orange arrows in Fig. 1. The remaining term is the antiferromagnetic Heisenberg interaction between the nearest neighbor layers.

By applying Holstein-Primakoff [113] and Fourier transformations, we can rewrite the Hamiltonian (1) as

$$\mathcal{H} = \frac{1}{2} \sum_{\mathbf{k}} [\mathbf{b}^\dagger(\mathbf{k}) \mathbf{b}(-\mathbf{k})] H(\mathbf{k}) \begin{bmatrix} \mathbf{b}(\mathbf{k}) \\ \mathbf{b}^\dagger(-\mathbf{k}) \end{bmatrix}, \quad (2)$$

where $\mathbf{b}(\mathbf{k}) = [b(\mathbf{k}, A, 1), b(\mathbf{k}, B, 1), b(\mathbf{k}, A, 2), b(\mathbf{k}, B, 2)]^T$. The operator $b(\mathbf{k}, A(B), 1(2))$ annihilates a magnon at the sublattice A(B) on the layer with odd (even) l . The matrix $H(\mathbf{k})$ is given in the Supplemental Material [114].

The Hamiltonian matrix has S symmetry: $S^{-1}(k_z) H(\mathbf{k}) S(k_z) = H(-\mathbf{k})$, where $S(k_z)$ is the combination operator defined by $S(k_z) = \Theta T_{1/2}(k_z)$. The time-reversal operator Θ and the translation of half a unit

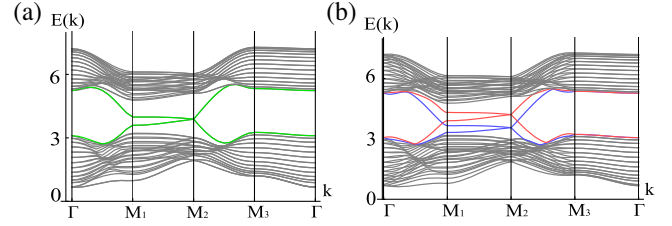


FIG. 2. (a) Magnon band structure of a slab with (100) face of stacked honeycomb lattice magnet, and (b) that under an electric field in the x direction. Topologically protected surface Dirac states are shown in (a) green and (b) red and blue. The parameters are $J_1^x = 1.6$, $J_1^y = 0.4$, $J_2^x = 1.0$, $J_2^y = 1.0$, $J_3^x = 0.4$, $J_3^y = 1.6$, $J_1^z = J_2^z = J_3^z = 1.1$, $D = 0.2$, $J' = 0.5$, and $S = 1.0$. Taking $\mathbf{a}_1 = (1, 0, 0)$, $\mathbf{a}_2 = (0, 1, 0)$ and $\mathbf{a}_3 = (0, 0, 1)$, we here deform the stacked honeycomb lattice into a topologically equivalent cubic-shaped lattice [114]. The symmetry points are $\Gamma = (0, 0)$, $M_1 = (\pi, 0)$, $M_2 = (\pi, \pi)$, $M_3 = (0, \pi)$.

cell in the z direction $T_{1/2}(k_z)$ are defined as $\Theta = K$ and $T_{1/2}(k_z) = 1_2 \otimes \sigma_x \text{diag}(1, e^{ik_z}) \otimes 1_2$ which satisfies $T_{1/2}(k_z)^2 = e^{ik_z}$, respectively. Here K , 1_2 , and σ_γ ($\gamma = x, y, z$), are the complex conjugation, the 2 by 2 identity matrix, and the Pauli matrices, respectively.

The equation $S(-k_z)S(k_z) = e^{ik_z}$ yields $S^2(\pi) = -1$, which leads to \mathbb{Z}_2 topological characterization in the same way as the magnonic analog of quantum spin Hall insulators [97]. Because of the Kramers theorem and the above relation, the bands of the model are doubly degenerate at time-reversal invariant momenta (TRIM) in the $k_z = \pi$ plane. As in Fig. 2(a), which shows the band structure of a slab with (100) face, a single Dirac cone can be found at $(k_y, k_z) = (\pi, \pi)$ (M_2 point). The situation is similar to that in strong topological insulators in class AII in the sense that a single Dirac cone appear. Then, the corresponding \mathbb{Z}_2 topological invariant of MAFTIs is defined as

$$\nu_{z,\pi}^{n\sigma} := \frac{1}{2\pi} \left[\oint_{\partial \text{EBZ}_{z,\pi}} d\mathbf{k} \cdot [\mathbf{A}_{n\sigma}(\mathbf{k})]_{k_z=\pi} - \int_{\text{EBZ}_{z,\pi}} dk_x dk_y [\Omega_{n\sigma}^z(\mathbf{k})]_{k_z=\pi} \right] \text{ mod } 2. \quad (3)$$

Here, we obtained Eq. (3) by replacing the pseudo-time-reversal operator Θ' with $S(\pi)$ in the definition of $\nu_{z,\pi}^{n\sigma}$ in Ref. [98]. We also confirmed the correspondence between the existence (absence) of Dirac surface states and $\nu_{z,\pi}^{n\sigma} = 1$ (0) by constructing the phase diagram of the model (1) [114]. We note that the first, second, and third terms of the Hamiltonian in Eq. (1) are all necessary [115] to realize the band structure having a single Dirac cone as in Fig. 2(a).

Energy current induced by a homogeneous electric field.—Next, we propose an intrinsic field response in MAFTIs, analogous to the topological magnetoelectric

effect [116–118] for electrons, whereas the mechanism is essentially different from that in electronic systems. Figure 2(b) represents the band structure of the model under an electric field $\mathbf{E} = E_x \mathbf{e}_x$. As shown in the figure, the electric field shifts dispersions on the surface states upward (red) and downward (blue). We will show that the imbalance of the dispersions of the surface states results in an energy current. This is an intrinsic phenomenon realized by the spin-momentum locking of the magnon surface states [101–103].

To understand the phenomena, let us consider the AC effect, in which magnons acquire a geometric phase by moving in an electric field \mathbf{E} . By applying an electric field, the vector potential $-(\sigma g \mu_B / c^2) \mathbf{E} \times \mathbf{e}_z$ is added to the wave vector of magnons:

$$\mathbf{k} \rightarrow \mathbf{k} - \frac{\sigma g \mu_B}{c^2} \mathbf{E} \times \mathbf{e}_z. \quad (4)$$

Here, c is the speed of light in a vacuum. The vector $-\sigma g \mu_B \mathbf{e}_z$ ($:= \boldsymbol{\mu}$) is the magnetic moment of magnons from up ($\sigma = +$) or down ($\sigma = -$) spins, where g is the g factor of the spins, μ_B is the Bohr magneton, and \mathbf{e}_γ ($\gamma = x, y, z$) is the unit vector in the γ direction.

Next, we show that the shift of the wave vector expressed by Eq. (4) gives rise to the shift of surface Dirac dispersions as in Fig. 2(b). We write the effective Hamiltonian with spin-momentum locking for $(\bar{1}00)$ and (100) surfaces as $H_+(\bar{\mathbf{k}})$ and $H_-(\bar{\mathbf{k}})$, respectively. Here, $\bar{\mathbf{k}}$ is defined as $\bar{\mathbf{k}} = (k_y, k_z)$. They can be written as follows:

$$H_\pm(\bar{\mathbf{k}}) = \pm \begin{pmatrix} \alpha k_y & \beta^* k_z \\ \beta k_z & -\alpha k_y \end{pmatrix}, \quad (5)$$

where the coefficients α and β are determined numerically (see Ref. [98] for the derivation). We note that the magnon state expressed by the wave function $\boldsymbol{\psi} = (1, 0)^T$ [$\boldsymbol{\psi}' = (0, 1)^T$] has the magnetic moment $\boldsymbol{\mu} = -g \mu_B \mathbf{e}_z$ ($\boldsymbol{\mu} = +g \mu_B \mathbf{e}_z$). The sign $+/-$ of $H_\pm(\bar{\mathbf{k}})$ corresponds to the chirality of the magnon Dirac surface state. By the Peierls substitution in Eq. (4), the effective Hamiltonian under a homogeneous electric field in the x direction $\mathbf{E} = E_x \mathbf{e}_x$ can be written as follows:

$$\begin{aligned} H_\pm(\bar{\mathbf{k}}) &\rightarrow \pm \begin{pmatrix} \alpha \left(k_y + \frac{g \mu_B}{c^2} E_x \right) & \beta^* k_z \\ \beta k_z & -\alpha \left(k_y - \frac{g \mu_B}{c^2} E_x \right) \end{pmatrix} \\ &= H_\pm(\bar{\mathbf{k}}) \pm \alpha \frac{g \mu_B}{c^2} E_x 1_2. \end{aligned} \quad (6)$$

Therefore, the energy of the gapless point of the Dirac state on $(\bar{1}00)$ surface shifts by $+\alpha(g \mu_B / c^2) E_x$, while the other shifts by $-\alpha(g \mu_B / c^2) E_x$.

To see the effect on these shifts, we introduce here the energy current operator defined as [42,119]

$$J_x = \sum_i \bar{P}_i \dot{h}_i, \quad (7)$$

where \bar{P}_i and \dot{h}_i are the position along the x direction and the time derivative of the Hamiltonian density at the site i , respectively. It can be rewritten as

$$J_x = \frac{1}{2} \sum_{\bar{\mathbf{k}}} \boldsymbol{\psi}^\dagger(\bar{\mathbf{k}}) J_x(\bar{\mathbf{k}}) \boldsymbol{\psi}(\bar{\mathbf{k}}), \quad (8)$$

where $\boldsymbol{\psi}(\bar{\mathbf{k}})$ is a set of magnon operators. The matrix $J_x(\bar{\mathbf{k}})$ is given by

$$J_x(\bar{\mathbf{k}}) = -\frac{i}{2} [\bar{P} H(\bar{\mathbf{k}}) \Sigma_z H(\bar{\mathbf{k}}) - H(\bar{\mathbf{k}}) \Sigma_z H(\bar{\mathbf{k}}) \bar{P}], \quad (9)$$

where $H(\bar{\mathbf{k}})$ and \bar{P} are the matrix forms of the Hamiltonian for a slab geometry with open boundary condition in the x direction and the position operator in the x direction, respectively. The matrix Σ_z is defined as $\Sigma_z = \sigma_z \otimes 1_{4N}$, where 1_{4N} is the $4N \times 4N$ identity matrix, and N is the number of the unit cells in the x direction parallel to the vector \mathbf{a}_1 . The details of the energy current operator are given in the Supplemental Material [114].

To evaluate the energy current induced by an electric field, we use the linear response theory, considering the field $E_x(t) = E_x e^{-i\omega t}$. Here, we describe the unperturbed Hamiltonian and the perturbation as H_0 and $H_E(t) = H_E e^{-i\omega t}$, respectively. The perturbation H_E is the Hamiltonian of the first order in the electric field E_x [114]. The expectation value of the energy current in the x direction J_x is given as follows:

$$\langle J_x \rangle = -\frac{i}{\hbar} \int_0^\infty d\tau e^{i\omega\tau} \text{tr} [e^{-iH_0\tau/\hbar} [H_E, \rho_0] e^{iH_0\tau/\hbar} J_x] e^{-i\omega t}, \quad (10)$$

where ρ_0 is the density operator for H_0 at thermal equilibrium. Hereafter, we use Planck units, i.e., the Planck constant $\hbar = 1$, the Boltzmann constant $k_B = 1$, and $c = 1$. In the limit of $\omega \rightarrow 0$, $\langle J_x \rangle$ is written as follows:

$$\begin{aligned} \langle J_x \rangle &= i \sum_{\bar{\mathbf{k}}} \sum_{\alpha\beta\gamma\delta\zeta\eta} \frac{n_B[E_\alpha(\bar{\mathbf{k}})] - n_B[E_\delta(\bar{\mathbf{k}})]}{[E_\alpha(\bar{\mathbf{k}}) - E_\delta(\bar{\mathbf{k}}) + i/\tau_\ell] [E_\alpha(\bar{\mathbf{k}}) - E_\delta(\bar{\mathbf{k}})]} \\ &\quad \times T_{\alpha\beta}^{-1}(\bar{\mathbf{k}}) (\hat{J}_x(\bar{\mathbf{k}}))_{\beta\gamma} T_{\gamma\delta}(\bar{\mathbf{k}}) T_{\delta\zeta}^{-1}(\bar{\mathbf{k}}) (\hat{H}_E(\bar{\mathbf{k}}))_{\zeta\eta} T_{\eta\alpha}(\bar{\mathbf{k}}), \end{aligned} \quad (11)$$

where n_B is the Bose distribution function. The matrices $\hat{J}_x(\bar{\mathbf{k}})$ and $\hat{H}_E(\bar{\mathbf{k}})$ are defined as $\hat{J}_x(\bar{\mathbf{k}}) = \Sigma_z J_x(\bar{\mathbf{k}})$ and $\hat{H}_E(\bar{\mathbf{k}}) = i[\Sigma_z H(\bar{\mathbf{k}}) \Sigma_z H_E(\bar{\mathbf{k}}) - \Sigma_z H_E(\bar{\mathbf{k}}) \Sigma_z H(\bar{\mathbf{k}})]$, respectively. The matrix $T(\bar{\mathbf{k}})$ is a paraunitary matrix satisfying $T(\bar{\mathbf{k}})^\dagger \Sigma_z T(\bar{\mathbf{k}}) = \Sigma_z$, which diagonalizes the magnon BdG

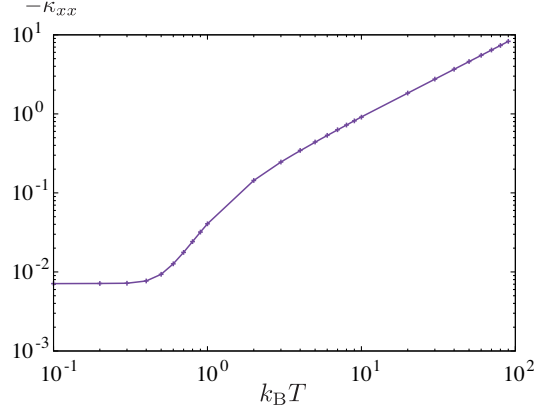


FIG. 3. Energy conductivity of the model (1) as a function of temperature. The data are calculated for $1/\tau_\ell = 10^{-2}$ and $N = 24$. We take the \vec{k} summation over 80×80 grid points in the Brillouin zone. The parameters are the same as those in Fig. 2.

Hamiltonian. Here, we introduce the phenomenological damping rate $1/\tau_\ell$ to take account of the finite lifetime of magnons.

Figure 3 shows the conductivity $\kappa_{xx} = \text{Re}[\langle J_x \rangle] / (g\mu_B E_x)$ as a function of temperature T . We can see that the conductivity is a monotonically increasing function of temperature. In the zero-temperature limit, κ_{xx} should become zero as magnons cannot be excited, whereas it appears to be nonzero. This is due to a finite size effect. We expect that the response discussed here is within the observable range because the AC phase due to an electric field has been observed in experiments, e.g., in a single-crystal yttrium iron garnet [120,121].

Another model: CrI₃.—Let us consider another model describing the magnetic compound CrI₃ [104–112] and point out that it is a candidate material for MAFTIs. Here, CrI₃ is a van der Waals material in which the magnetic moments are carried by Cr³⁺ ions with electronic configuration $3d^3$ forming a honeycomb lattice structure. The spin magnitude of each Cr³⁺ ion is $S = 3/2$. The crystal structure of the stacked honeycomb lattice magnet CrI₃ is monoclinic (rhombohedral) at a high (low) temperature. The Hamiltonian of CrI₃ with the monoclinic structure illustrated in Fig. 4(a) is given by

$$\begin{aligned} \mathcal{H} = & \sum_l \sum_{\gamma=x,y,z} \sum_{\langle ij \rangle_\gamma} H'_{ij,l} + D \sum_{\langle\langle ij \rangle\rangle_l} \xi_{ij} (\mathbf{S}_{i,l} \times \mathbf{S}_{j,l})_z \\ & + J' \sum_{\langle\langle i,l \rangle\rangle, \langle\langle j,l' \rangle\rangle \in \text{mono}} \mathbf{S}_{i,l} \cdot \mathbf{S}_{j,l'} - \kappa \sum_i (S_i^z)^2. \end{aligned} \quad (12)$$

Here, $\langle ij \rangle_\gamma$ ($\gamma = x, y, z$) denotes a pair of the nearest neighbor sites i and j on the x , y , and z bonds which are colored with red, green, and blue in Fig. 4(a), respectively. The contribution from the z bond in the l th layer is written as

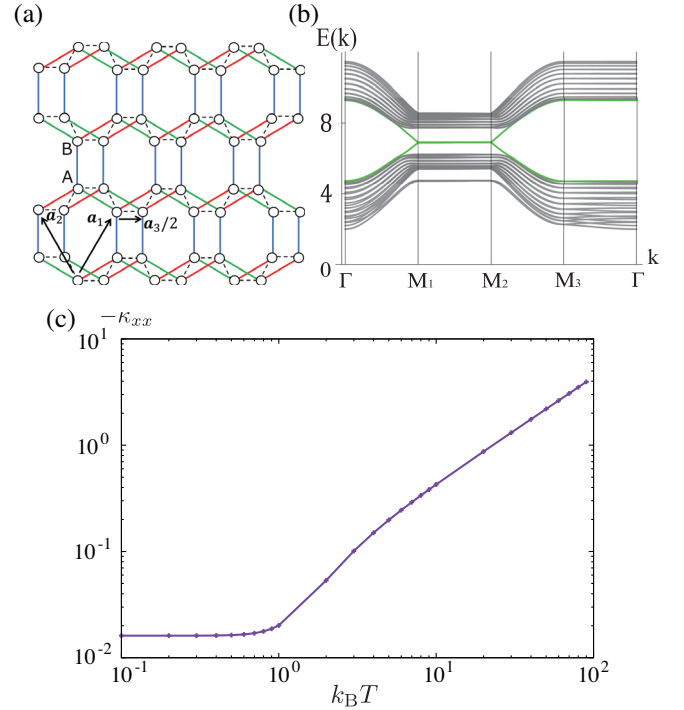


FIG. 4. (a) Monoclinic honeycomb-layer stacking structure of CrI₃. Red, green, and blue bonds on the honeycomb lattice are the x , y , and z bonds, respectively. The black dashed lines represent the couplings of the third term in Eq. (12). The spins in odd and even layers point upward and downward, respectively, as in Fig. 1. The lattice primitive vectors are written as \mathbf{a}_1 , \mathbf{a}_2 , and \mathbf{a}_3 . The arrows along the horizontal black dashed lines correspond to $\mathbf{a}_3/2$. (b) The magnon band structure of a slab with (100) face of the model (12). Topologically protected Dirac states are shown in green. (c) Energy conductivity of the model (12) as a function of temperature. The parameters for (b) and (c) are $J = 1.0$, $K = -0.5$, $\Gamma = 0.3$, $D = 0.07$, $J' = 0.1$, $\kappa = 0.4$, and $S = 3/2$. We set $1/\tau_\ell = 10^{-2}$, $N = 24$, and take the \vec{k} summation over 80×80 grid points in (c).

$$H_{ij,l}^z = -JS_{i,l} \cdot \mathbf{S}_{j,l} + KS_{i,l}^z S_{j,l}^z + \Gamma(S_{i,l}^x S_{j,l}^y + S_{i,l}^y S_{j,l}^x). \quad (13)$$

The first and second terms in Eq. (13) are the ferromagnetic Heisenberg and Kitaev interactions, respectively. The third term is the symmetric off-diagonal intralayer interaction. We can obtain the contributions from the x and y bonds ($H_{ij,l}^x$ and $H_{ij,l}^y$) by a cyclic permutation among S^x , S^y , and S^z . The second term in Eq. (12) represents the DM interaction between intralayer next-nearest neighbor sites. The remaining terms are the antiferromagnetic Heisenberg interaction between the nearest-neighbor layers and the easy axis anisotropy. The summation $\sum_{\langle\langle i,l \rangle\rangle, \langle\langle j,l' \rangle\rangle \in \text{mono}}$ is taken over the nearest-neighbor bonds across the layers in the monoclinic structure, which are shown in the black dashed lines in Fig. 4(a). The magnon Hamiltonian of the model is given in the Supplemental Material [114].

Figure 4(b) shows the band structure for the model (12) of a slab with (100) face. We can find a single Dirac cone at M_2 point while the surface states are nearly degenerate from M_1 to M_2 . Here, we used the parameters estimated by density functional theory calculations for CrI_3 [109,124]. Since the band split between M_1 and M_2 comes from the Γ interaction which breaks spin conservation and the inter-layer coupling, we can see a more distinct single Dirac cone when Γ and J' are larger. The surface states are protected by S symmetry, and then they shift upward and downward under an electric field via the spin-momentum locking, as in Fig. 2(b). As discussed in the previous section, such a system exhibits the energy current induced by an electric field. Figure 4(c) shows the energy conductivity κ_{xx} as a function of temperature T . The behavior is similar to that in the model (1) [see Fig. 3], while the starting points of the increase are different due to the difference between the heights of the magnon bands. We also confirm that such a topological phase appears in a wide range of parameters by constructing a phase diagram of the model (12) [114].

Summary.—In this Letter, we have constructed a model for a magnet which has surface states of magnons protected by the combined symmetry of time-reversal and half translation. The single Dirac surface states of the system appear as in the strong topological insulators in class AII, and thus it is expected to be robust against disorder as long as the respected symmetry is preserved [125]. We have also demonstrated that an electric field shifts the position of the Dirac cones in one and the other surfaces oppositely, resulting in an energy current. So far, the AC effect of magnons in a homogeneous electric field has not attracted much attention since the outcome is merely the shift of the wave vector in most cases. However, our study has revealed that nontrivial response in magnon systems to a homogeneous electric field could be realized by the presence of topologically protected surface states and the interactions which break conservation of S_z . A promising candidate material which exhibits this physics could be CrI_3 with a monoclinic structure. Although the structure is realized at a temperature higher than 200 K, it has been reported that the monoclinic structure remains unchanged in a thin film of CrI_3 even when the temperature is lowered below 200 K [110]. We expect the magnon physics discussed in this Letter can be realized in a thin film of CrI_3 , and similar materials. Observation of the (shift of) Dirac surface states and magnon current under an electric field would provide the smoking-gun evidence for the realization of the topological phase, MAFTI.

We thank Hosho Katsura for valuable discussions and helpful comments on the manuscript. This work was supported by JSPS KAKENHI Grants No. JP17K14352, No. JP20K14411, No. JP20J12861, and JSPS Grant-in-Aid for Scientific Research on Innovative Areas “Topological Materials Science” (KAKENHI Grant No. JP18H04220) and “Quantum Liquid Crystals” (KAKENHI Grant No. JP20H05154). H. K. was supported by the JSPS through Program for Leading Graduate Schools

[Advanced Leading Graduate Course for Photon Science (ALPS)]. Y. A. also thanks the Okinawa Institute of Science and Technology Graduate University for the use of the facilities, Deigo cluster.

*kondo-hiroki290@g.ecc.u-tokyo.ac.jp

- [1] K. v. Klitzing, G. Dorda, and M. Pepper, *Phys. Rev. Lett.* **45**, 494 (1980).
- [2] D. J. Thouless, M. Kohmoto, M. P. Nightingale, and M. den Nijs, *Phys. Rev. Lett.* **49**, 405 (1982).
- [3] M. Kohmoto, *Ann. Phys. (N.Y.)* **160**, 343 (1985).
- [4] A. P. Schnyder, S. Ryu, A. Furusaki, and A. W. W. Ludwig, *Phys. Rev. B* **78**, 195125 (2008).
- [5] A. Kitaev, *AIP Conf. Proc.* **1134**, 22 (2009).
- [6] S. Ryu, A. P. Schnyder, A. Furusaki, and A. W. W. Ludwig, *New J. Phys.* **12**, 065010 (2010).
- [7] M. Z. Hasan and C. L. Kane, *Rev. Mod. Phys.* **82**, 3045 (2010).
- [8] X.-L. Qi and S.-C. Zhang, *Rev. Mod. Phys.* **83**, 1057 (2011).
- [9] C. L. Kane and E. J. Mele, *Phys. Rev. Lett.* **95**, 226801 (2005).
- [10] C. L. Kane and E. J. Mele, *Phys. Rev. Lett.* **95**, 146802 (2005).
- [11] L. Fu, C. L. Kane, and E. J. Mele, *Phys. Rev. Lett.* **98**, 106803 (2007).
- [12] D. N. Sheng, Z. Y. Weng, L. Sheng, and F. D. M. Haldane, *Phys. Rev. Lett.* **97**, 036808 (2006).
- [13] K. Nomura, M. Koshino, and S. Ryu, *Phys. Rev. Lett.* **99**, 146806 (2007).
- [14] H. Obuse, A. Furusaki, S. Ryu, and C. Mudry, *Phys. Rev. B* **76**, 075301 (2007).
- [15] A. M. Essin and J. E. Moore, *Phys. Rev. B* **76**, 165307 (2007).
- [16] H. Jiang, L. Wang, Q.-f. Sun, and X. C. Xie, *Phys. Rev. B* **80**, 165316 (2009).
- [17] J. Li, R.-L. Chu, J. K. Jain, and S.-Q. Shen, *Phys. Rev. Lett.* **102**, 136806 (2009).
- [18] C. W. Groth, M. Wimmer, A. R. Akhmerov, J. Tworzydło, and C. W. J. Beenakker, *Phys. Rev. Lett.* **103**, 196805 (2009).
- [19] H.-M. Guo, *Phys. Rev. B* **82**, 115122 (2010).
- [20] T. A. Loring and M. B. Hastings, *Europhys. Lett.* **92**, 67004 (2010).
- [21] E. Prodan, *Phys. Rev. B* **83**, 195119 (2011).
- [22] A. Yamakage, K. Nomura, K.-I. Imura, and Y. Kuramoto, *J. Phys. Soc. Jpn.* **80**, 053703 (2011).
- [23] I. C. Fulga, F. Hassler, and A. R. Akhmerov, *Phys. Rev. B* **85**, 165409 (2012).
- [24] B. Leung and E. Prodan, *Phys. Rev. B* **85**, 205136 (2012).
- [25] K. Kobayashi, T. Ohtsuki, and K.-I. Imura, *Phys. Rev. Lett.* **110**, 236803 (2013).
- [26] B. Sbierski and P. W. Brouwer, *Phys. Rev. B* **89**, 155311 (2014).
- [27] H. Katsura and T. Koma, *J. Math. Phys. (N.Y.)* **57**, 021903 (2016).
- [28] Y. Akagi, H. Katsura, and T. Koma, *J. Phys. Soc. Jpn.* **86**, 123710 (2017).

- [29] H. Katsura and T. Koma, *J. Math. Phys. (N.Y.)* **59**, 031903 (2018).
- [30] L. Fu, *Phys. Rev. Lett.* **106**, 106802 (2011).
- [31] Y. Tanaka, Z. Ren, T. Sato, K. Nakayama, S. Souma, T. Takahashi, K. Segawa, and Y. Ando, *Nat. Phys.* **8**, 800 (2012).
- [32] P. Dziawa, B. J. Kowalski, K. Dybko, R. Buczko, A. Szczerbakow, M. Szot, E. usakowska, T. Balasubramanian, B. M. Wojek, M. H. Berntsen, O. Tjernberg, and T. Story, *Nat. Mater.* **11**, 1023 (2012).
- [33] K. Shiozaki and M. Sato, *Phys. Rev. B* **90**, 165114 (2014).
- [34] R. S. K. Mong, A. M. Essin, and J. E. Moore, *Phys. Rev. B* **81**, 245209 (2010).
- [35] S. Fujimoto, *Phys. Rev. Lett.* **103**, 047203 (2009).
- [36] H. Katsura, N. Nagaosa, and P. A. Lee, *Phys. Rev. Lett.* **104**, 066403 (2010).
- [37] Y. Onose, T. Ideue, H. Katsura, Y. Shiomi, N. Nagaosa, and Y. Tokura, *Science* **329**, 297 (2010).
- [38] R. Matsumoto and S. Murakami, *Phys. Rev. B* **84**, 184406 (2011).
- [39] T. Ideue, Y. Onose, H. Katsura, Y. Shiomi, S. Ishiwata, N. Nagaosa, and Y. Tokura, *Phys. Rev. B* **85**, 134411 (2012).
- [40] R. Shindou, J. I. Ohe, R. Matsumoto, S. Murakami, and E. Saitoh, *Phys. Rev. B* **87**, 174402 (2013).
- [41] R. Shindou, R. Matsumoto, S. Murakami, and J. I. Ohe, *Phys. Rev. B* **87**, 174427 (2013).
- [42] R. Matsumoto, R. Shindou, and S. Murakami, *Phys. Rev. B* **89**, 054420 (2014).
- [43] R. Chisnell, J. S. Helton, D. E. Freedman, D. K. Singh, R. I. Bewley, D. G. Nocera, and Y. S. Lee, *Phys. Rev. Lett.* **115**, 147201 (2015).
- [44] M. Hirschberger, R. Chisnell, Y. S. Lee, and N. P. Ong, *Phys. Rev. Lett.* **115**, 106603 (2015).
- [45] S. K. Kim, H. Ochoa, R. Zarzuela, and Y. Tserkovnyak, *Phys. Rev. Lett.* **117**, 227201 (2016).
- [46] J. H. Han and H. Lee, *J. Phys. Soc. Jpn.* **86**, 011007 (2017).
- [47] S. Murakami and A. Okamoto, *J. Phys. Soc. Jpn.* **86**, 011010 (2017).
- [48] K. Li, C. Li, J. Hu, Y. Li, and C. Fang, *Phys. Rev. Lett.* **119**, 247202 (2017).
- [49] S. S. Pershoguba, S. Banerjee, J. C. Lashley, J. Park, H. Ågren, G. Aeppli, and A. V. Balatsky, *Phys. Rev. X* **8**, 011010 (2018).
- [50] B. Li and A. A. Kovalev, *Phys. Rev. B* **97**, 174413 (2018).
- [51] S. Bao, J. Wang, W. Wang, Z. Cai, S. Li, Z. Ma, D. Wang, K. Ran, Z.-Y. Dong, D. L. Abernathy, S.-L. Yu, X. Wan, J.-X. Li, and J. Wen, *Nat. Commun.* **9**, 2591 (2018).
- [52] M. Kawano and C. Hotta, *Phys. Rev. B* **99**, 054422 (2019).
- [53] M. Onoda, S. Murakami, and N. Nagaosa, *Phys. Rev. Lett.* **93**, 083901 (2004).
- [54] S. Raghu and F. D. M. Haldane, *Phys. Rev. A* **78**, 033834 (2008).
- [55] F. D. M. Haldane and S. Raghu, *Phys. Rev. Lett.* **100**, 013904 (2008).
- [56] O. Hosten and P. Kwiat, *Science* **319**, 787 (2008).
- [57] Z. Wang, Y. Chong, J. D. Joannopoulos, and M. Soljačić, *Nature (London)* **461**, 772 (2009).
- [58] L. Lu, L. Fu, J. D. Joannopoulos, and M. Soljačić, *Nat. Photonics* **7**, 294 (2013).
- [59] P. Ben-Abdallah, *Phys. Rev. Lett.* **116**, 084301 (2016).
- [60] C. Strohm, G. L. J. A. Rikken, and P. Wyder, *Phys. Rev. Lett.* **95**, 155901 (2005).
- [61] L. Sheng, D. N. Sheng, and C. S. Ting, *Phys. Rev. Lett.* **96**, 155901 (2006).
- [62] A. V. Inyushkin and A. N. Taldenkov, *JETP Lett.* **86**, 379 (2007).
- [63] Y. Kagan and L. A. Maksimov, *Phys. Rev. Lett.* **100**, 145902 (2008).
- [64] J.-S. Wang and L. Zhang, *Phys. Rev. B* **80**, 012301 (2009).
- [65] L. Zhang, J. Ren, J.-S. Wang, and B. Li, *Phys. Rev. Lett.* **105**, 225901 (2010).
- [66] T. Qin, J. Zhou, and J. Shi, *Phys. Rev. B* **86**, 104305 (2012).
- [67] R. Süssstrunk and S. D. Huber, *Science* **349**, 47 (2015).
- [68] O. Stenull, C. L. Kane, and T. C. Lubensky, *Phys. Rev. Lett.* **117**, 068001 (2016).
- [69] R. Süssstrunk and S. D. Huber, *Proc. Natl. Acad. Sci. U.S.A.* **113**, E4767 (2016).
- [70] M. Mori, A. Spencer-Smith, O. P. Sushkov, and S. Maekawa, *Phys. Rev. Lett.* **113**, 265901 (2014).
- [71] K. Sugii, M. Shimozawa, D. Watanabe, Y. Suzuki, M. Halim, M. Kimata, Y. Matsumoto, S. Nakatsuji, and M. Yamashita, *Phys. Rev. Lett.* **118**, 145902 (2017).
- [72] J. Rumhányi, K. Penc, and R. Ganesh, *Nat. Commun.* **6**, 6805 (2015).
- [73] P. A. McClarty, F. Krüger, T. Guidi, S. F. Parker, K. Refson, A. W. Parker, D. Prabhakaran, and R. Coldea, *Nat. Phys.* **13**, 736 (2017).
- [74] D. G. Joshi and A. P. Schnyder, *Phys. Rev. B* **96**, 220405 (R) (2017).
- [75] D. G. Joshi and A. P. Schnyder, *Phys. Rev. B* **100**, 020407 (R) (2019).
- [76] K. Nawa, K. Tanaka, N. Kurita, T. J. Sato, H. Sugiyama, H. Uekusa, S. Ohira-Kawamura, K. Nakajima, and H. Tanaka, *Nat. Commun.* **10**, 2096 (2019).
- [77] A. Thomasen, K. Penc, N. Shannon, and J. Romhányi, *Phys. Rev. B* **104**, 104412 (2021).
- [78] S. Furukawa and M. Ueda, *New J. Phys.* **17**, 115014 (2015).
- [79] G. Engelhardt and T. Brandes, *Phys. Rev. A* **91**, 053621 (2015).
- [80] C.-E. Bardyn, T. Karzig, G. Refael, and T. C. H. Liew, *Phys. Rev. B* **93**, 020502(R) (2016).
- [81] Z.-F. Xu, L. You, A. Hemmerich, and W. V. Liu, *Phys. Rev. Lett.* **117**, 085301 (2016).
- [82] M. Di Liberto, A. Hemmerich, and C. Morais Smith, *Phys. Rev. Lett.* **117**, 163001 (2016).
- [83] J.-S. Pan, W. Zhang, W. Yi, and G.-C. Guo, *Phys. Rev. A* **94**, 043619 (2016).
- [84] G.-Q. Luo, A. Hemmerich, and Z.-F. Xu, *Phys. Rev. A* **98**, 053617 (2018).
- [85] T. Yoshino, S. Furukawa, S. Higashikawa, and M. Ueda, *New J. Phys.* **21**, 015001 (2019).
- [86] T. Ohashi, S. Kobayashi, and Y. Kawaguchi, *Phys. Rev. A* **101**, 013625 (2020).
- [87] S. Lieu, *Phys. Rev. B* **98**, 115135 (2018).

- [88] K. Kawabata, K. Shiozaki, M. Ueda, and M. Sato, *Phys. Rev. X* **9**, 041015 (2019).
- [89] H. Kondo, Y. Akagi, and H. Katsura, *Prog. Theor. Exp. Phys.* **2020**, 12A104 (2020).
- [90] F.-Y. Li, Y.-D. Li, Y. B. Kim, L. Balents, Y. Yu, and G. Chen, *Nat. Commun.* **7**, 12691 (2016).
- [91] A. Mook, J. Henk, and I. Mertig, *Phys. Rev. Lett.* **117**, 157204 (2016).
- [92] S. A. Owerre, *Phys. Rev. B* **97**, 094412 (2018).
- [93] Y. Su, X. S. Wang, and X. R. Wang, *Phys. Rev. B* **95**, 224403 (2017).
- [94] T. Liu and Z. Shi, *Phys. Rev. B* **99**, 214413 (2019).
- [95] V. A. Zyuzin and A. A. Kovalev, *Phys. Rev. Lett.* **117**, 217203 (2016).
- [96] K. Nakata, S. K. Kim, J. Klinovaja, and D. Loss, *Phys. Rev. B* **96**, 224414 (2017).
- [97] H. Kondo, Y. Akagi, and H. Katsura, *Phys. Rev. B* **99**, 041110(R) (2019).
- [98] H. Kondo, Y. Akagi, and H. Katsura, *Phys. Rev. B* **100**, 144401 (2019).
- [99] In the models for the magnonic analog of topological insulators in three dimensions [98], two spins are localized at each site of the diamond lattice and point in opposite directions. In addition, fine-tuning of quite complicated interactions is required to realize the topological phase.
- [100] Y. Aharonov and A. Casher, *Phys. Rev. Lett.* **53**, 319 (1984).
- [101] N. Okuma, *Phys. Rev. Lett.* **119**, 107205 (2017).
- [102] M. Kawano, Y. Onose, and C. Hotta, *Commun. Phys.* **2**, 27 (2019).
- [103] M. Kawano and C. Hotta, *Phys. Rev. B* **100**, 174402 (2019).
- [104] M. A. McGuire, H. Dixit, V. R. Cooper, and B. C. Sales, *Chem. Mater.* **27**, 612 (2015).
- [105] B. Huang, G. Clark, E. Navarro-Moratalla, D. R. Klein, R. Cheng, K. L. Seyler, D. Zhong, E. Schmidgall, M. A. McGuire, D. H. Cobden, W. Yao, D. Xiao, P. Jarillo-Herrero, and X. Xu, *Nature (London)* **546**, 270 (2017).
- [106] B. Huang, G. Clark, D. R. Klein, D. MacNeill, E. Navarro-Moratalla, K. L. Seyler, N. Wilson, M. A. McGuire, D. H. Cobden, D. Xiao, W. Yao, P. Jarillo-Herrero, and X. Xu, *Nat. Nanotechnol.* **13**, 544 (2018).
- [107] L. Chen, J.-H. Chung, B. Gao, T. Chen, M. B. Stone, A. I. Kolesnikov, Q. Huang, and P. Dai, *Phys. Rev. X* **8**, 041028 (2018).
- [108] N. Sivadas, S. Okamoto, X. Xu, C. J. Fennie, and D. Xiao, *Nano Lett.* **18**, 7658 (2018).
- [109] D. Soriano, C. Cardoso, and J. Fernández-Rossier, *Solid State Commun.* **299**, 113662 (2019).
- [110] N. Ubrig, Z. Wang, J. Teyssier, T. Taniguchi, K. Watanabe, E. Giannini, A. F. Morpurgo, and M. Gibertini, *2D Mater.* **7**, 015007 (2019).
- [111] A. T. Costa, D. L. R. Santos, N. M. R. Peres, and J. Fernández-Rossier, *2D Mater.* **7**, 045031 (2020).
- [112] D. Soriano, M. I. Katsnelson, and J. Fernández-Rossier, *Nano Lett.* **20**, 6225 (2020).
- [113] T. Holstein and H. Primakoff, *Phys. Rev.* **58**, 1098 (1940).
- [114] See Supplemental Material at <http://link.aps.org/supplemental/10.1103/PhysRevLett.127.177201> for details of the explicit expression of magnon Hamiltonians, the perturbation Hamiltonian, the energy current operator. It also provides the details of the topologically equivalent lattice deformation and the phase diagrams for the models (1) and (12) in the main text.
- [115] The DM interaction plays a role in making the magnon bands topologically nontrivial. The XYZ anisotropy, which breaks spin conservation, and bond dependence of the Heisenberg interaction lift the degeneracy of surface states from M_1 to M_2 points, resulting in a single Dirac cone at M_2 point. It is also noted that without the interlayer interaction, the system would be merely stacked Chern insulators of magnons with alternating Chern numbers.
- [116] X. L. Qi, T. L. Hughes, and S. C. Zhang, *Phys. Rev. B* **78**, 195424 (2008).
- [117] K. Nomura and N. Nagaosa, *Phys. Rev. Lett.* **106**, 166802 (2011).
- [118] T. Morimoto, A. Furusaki, and N. Nagaosa, *Phys. Rev. B* **92**, 085113 (2015).
- [119] I. Paul and G. Kotliar, *Phys. Rev. B* **67**, 115131 (2003).
- [120] X. Zhang, T. Liu, M. E. Flatté, and H. X. Tang, *Phys. Rev. Lett.* **113**, 037202 (2014).
- [121] The AC phase of magnons can also be understood in terms of electric-field-induced DM interaction (via the spin-orbit interaction) due to the superexchange mechanism [122,123], which is proportional to the strength of the electric field. In fact, the form of the phase is identical to that of the AC phase, and thus they are indistinguishable from each other. The spin-orbit interaction itself induced by an electric field in a vacuum is quite small. However, the interaction can be drastically enhanced in solids as we observed a variety of phenomena originating from the spin-orbit interaction.
- [122] T. Liu and G. Vignale, *Phys. Rev. Lett.* **106**, 247203 (2011).
- [123] H. Katsura, N. Nagaosa, and A. V. Balatsky, *Phys. Rev. Lett.* **95**, 057205 (2005).
- [124] Y. O. Kvashnin, A. Bergman, A. I. Lichtenstein, and M. I. Katsnelson, *Phys. Rev. B* **102**, 115162 (2020).
- [125] It has been verified that magnon topological phases with a nontrivial Chern number is robust against disorder: B. Xu, T. Ohtsuki, and R. Shindou, *Phys. Rev. B* **94**, 220403(R) (2016); X. S. Wang, A. Brataas, and R. E. Troncoso, *Phys. Rev. Lett.* **125**, 217202 (2020); Y. Akagi, *J. Phys. Soc. Jpn.* **89**, 123601 (2020).